

$\Lambda(1405, 1/2^-)$ photoproduction from the $\gamma p \rightarrow K^+ \Lambda(1405)$ reaction

Seung-il Nam,^{1,*} Ji-Hyoung Park,^{2,†} Atsushi Hosaka,^{3,‡} and Hyun-Chul Kim^{4,§}

¹*Research Institute of Basic Sciences, Korea Aerospace University, Goyang, 412-791, Korea*

²*Department of Physics, Pusan National University, Busan 609-735, Republic of Korea*

³*Research Center for Nuclear Physics (RCNP), Ibaraki, Osaka 567-0047, Japan*

⁴*Department of Physics, Inha University, Incheon 402-751, Republic of Korea*

(Dated: June, 2011)

We investigate the photoproduction of $\Lambda(1405, 1/2^-) \equiv \Lambda^*$ off the proton target using the effective Lagrangian in the Born approximation. We observed that, depending on the choice of the $K^* N \Lambda^*$ coupling strength, the total cross section becomes $0.1 \lesssim \sigma_{\Lambda^*} \lesssim 0.2 \mu\text{b}$ near the threshold and starts to decrease beyond $E_\gamma \approx 1.6$ GeV, and the angular dependence shows a mild enhancement in the forward direction. It turns out that the energy dependence of the total cross section is similar to that shown in the recent LEPS experiment. This suggests that the production mechanism of the Λ^* is dominated by the *s*-channel contribution.

PACS numbers: 13.60.Le, 14.20.Jn

Keywords: $\Lambda(1405)$ photoproduction, effective Lagrangian method, *s*-channel dominance

I. INTRODUCTION

The $\Lambda(1405, 1/2^-) \equiv \Lambda^*$, an excited state of the $\Lambda(1116, 1/2^+)$ with negative parity, has been studied for decades (See Ref. [1] for the review until 1998). Its production has been mainly conducted in proton-proton scattering and meson-proton scattering. Recently, however, the LEPS collaboration has carried out the measurement of the Λ^* produced in the $\gamma p \rightarrow K^+ \Lambda^*$ reaction [2, 3]. While for the ground state $\Lambda(1116, 1/2^+)$ and for the *d*-wave $\Lambda(1520, 3/2^-)$ photoproductions, there are many experimental data [4, 5] as well as theoretical investigations [6–10], there has been only a few theoretical works on the Λ^* photoproduction to date [11–13] and related experiments mainly performed by the LEPS collaboration at SPring-8 [2, 3].

Nevertheless, there are several interesting theoretical works. For example, Ref. [11] estimated the differential cross section for the $\gamma p \rightarrow K^+ \Lambda^*$ reaction, considering the crossing symmetry and duality, whereas Refs. [12, 13] concentrated on the Λ^* invariant mass spectrum via the $\gamma p \rightarrow K^+ \pi \Sigma$ scattering process using the *s*-wave chiral dynamics, also known as the chiral unitary model (χ UM), in which the Λ^* is assumed to be the molecular-type $\bar{K}N$ state rather than a three-quark color-singlet (*uds*) one such as usual baryons. In the recent LEPS experiment [2], interestingly, it turned out that the $\Lambda^*/\Sigma(1385)$ production ratio is very different between the low ($1.5 \lesssim E_\gamma \lesssim 2.0$ GeV) and high ($2.0 \lesssim E_\gamma \lesssim 2.4$ GeV) energy regions. It implies that the total cross section for the Λ^* increases near the threshold, and then starts to decrease as the photon energy is increased. It was suggested that this interesting tendency may be caused by either the different production mechanisms from that for the $\Sigma(1385)$ or the novel internal structure of the Λ^* .

In the present work, we aim at investigating the $\gamma p \rightarrow K^+ \Lambda^*$ reaction, using the effective Lagrangian in the Born approximation. We make use of theoretical and experimental information to determine relevant parameters such as the coupling strengths and cutoff masses for the phenomenological form factors, which are treated in a gauge-invariant manner. By changing the cutoff mass for the phenomenological form factor for the $\gamma \Lambda^* \Lambda^*$ vertex, the size effect, which may encode the internal structure of the Λ^* , is examined.

We observe that, depending on the choice of the $K^* N \Lambda^*$ coupling strength, the total cross section becomes $0.1 \lesssim \sigma_{\Lambda^*} \lesssim 0.2 \mu\text{b}$ near the threshold and starts to decrease slowly beyond $E_\gamma \approx 1.6$ GeV, and the angular dependence shows a mild enhancement in the forward direction. It is also found that the size effect of the Λ^* is seen mainly due to the *u*-channel near the threshold but very small. Comparing these results to the experimental data [2], the overall energy dependence of the σ_{Λ^*} is very similar. This indicates that the production mechanism of the Λ^* is dominated

*E-mail: sinam@kau.ac.kr

†E-mail: parkjihyoung@pusan.ac.kr

‡E-mail: hosaka@rcnp.osaka-u.ac.jp

§E-mail: hchkim@inha.ac.kr

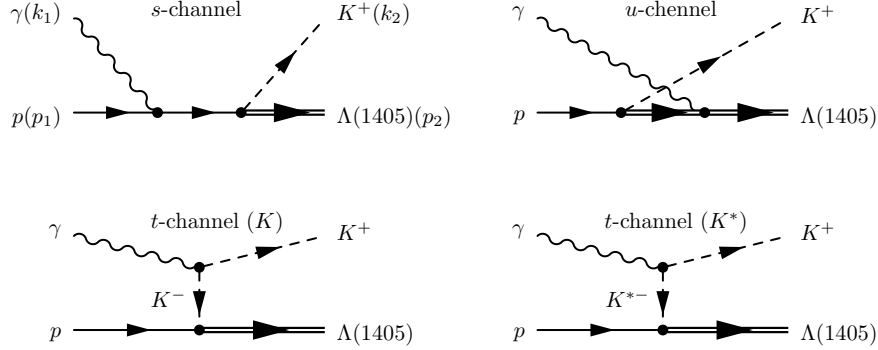


FIG. 1: Feynman diagrams for the Λ^* photoproduction from the proton target, $\gamma p \rightarrow K^+ \Lambda(1405)$, in the pseudoscalar (PS) meson-baryon coupling scheme.

by the *s*-channel contribution rather than the *t*-channel one. The photon-beam asymmetry shows a strong electric photon-hadron coupling contribution due to the *t*-channel.

We organize the present work as follows: In Section II, we briefly explain the general formalism relevant for studying the $\gamma p \rightarrow K^+ \Lambda^*$ scattering process. In Section III, the numerical results are given with discussions. Theoretical ambiguities are briefly explained in Section IV. The final Section is devoted to summarize the present work and to draw conclusions.

II. GENERAL FORMALISM

We start with the general formalism for the $\Lambda(1405, 1/2^-) \equiv \Lambda^*$ photoproduction. In Fig. 1, we depict the relevant Feynman diagrams. The four momenta for the involved particles are defined in the figure. To compute the diagrams, we employ the following effective Lagrangian in the pseudoscalar (PS) meson-baryon coupling scheme:

$$\begin{aligned}
 \mathcal{L}_{\gamma KK} &= ie_K [(\partial^\mu K^\dagger)K - (\partial^\mu K)K^\dagger] A_\mu + \text{h.c.}, \\
 \mathcal{L}_{\gamma NN} &= -\bar{N} \left[e_N A + \frac{\kappa_N}{2M_N} \sigma_{\mu\nu} F^{\mu\nu} \right] N + \text{h.c.}, \\
 \mathcal{L}_{\gamma \Lambda^* \Lambda^*} &= -\frac{\kappa_{\Lambda^*}}{2M_{\Lambda^*}} \bar{\Lambda}^* \sigma_{\mu\nu} F^{\mu\nu} \Lambda^* + \text{h.c.}, \\
 \mathcal{L}_{K N \Lambda^*} &= ig_{K N \Lambda^*} \bar{\Lambda}^* K^\dagger N + \text{h.c.}, \\
 \mathcal{L}_{\gamma K K^*} &= g_{\gamma K K^*} \epsilon_{\mu\nu\sigma\rho} (\partial^\mu A^\nu) (\partial^\sigma K^\dagger) K^{*\rho} + \text{h.c.}, \\
 \mathcal{L}_{K^* N \Lambda^*} &= g_{K^* N \Lambda^*} \bar{\Lambda}^* \gamma^\mu \gamma_5 K_\mu^{*\dagger} N + \text{h.c.},
 \end{aligned} \tag{1}$$

where K , A_μ , N , Λ^* , and K^* represent the pseudoscalar kaon, photon, nucleon, Λ^* , and vector kaon fields, respectively. The e_h , κ_h , and M_h denote the electric charge, the anomalous magnetic moment, and the mass, respectively, corresponding to the hadron h . As for the K^* -exchange contribution, we neglect the tensor coupling of the $K^* N \Lambda^*$ vertex, assuming its strength to be small.

Above the threshold energy $E_\gamma \simeq 1900$ MeV, there are eight nucleon resonances (N^*), as reported in Ref. [14], up to $\sqrt{s} \simeq 2200$ MeV: $P_{13}(1900)$, $F_{17}(1990)$, $F_{15}(2000)$, $D_{13}(2080)$, $S_{11}(2090)$, $P_{11}(2100)$, $G_{17}(2190)$, $D_{15}(2200)$. Except for the G_{17} , their confirmations are still poor (below two stars). Moreover, we have little knowledge about the $N^* \rightarrow K \Lambda^*$ decay process in comparison to other hyperons. Hence, we exclude these resonance contributions not to increase theoretical ambiguities for the moment.

We now discuss how to determine the coupling strength of the $g_{K N \Lambda^*}$ briefly. Although the Λ^* does not decay into $\bar{K} N$ in free space, the value of the $g_{K N \Lambda^*}$ was estimated within the potential model and chiral unitary model (χ UM) [12, 15, 16]. In the χ UM, it was argued that the Λ^* may consist of two individual poles [12, 16]. The pole positions are $1398 - 74i$ MeV (lower one) and $1429 - 14i$ (higher one) in the dimensional regularization scheme [15]. The coupling strengths to these poles were obtained from the residue of the amplitude, resulting in $g_{K N \Lambda^*} = 1.43$

for the lower pole and $g_{K\Lambda^*} = 2.52$ for the higher one in the dimensional regularization¹. When the dipole- and monopole-type form factors are applied to the regularization of the loop integral, one has $g_{K\Lambda^*} = 2.00$ and 3.64 , whereas 2.65 and 3.39 , respectively [15]. Considering that the higher pole couples strongly to the $\bar{K}N$ state, we take the average of those values of $g_{K\Lambda^*}$, resulting in 3.18 . This value is not much different from $1.5 \sim 3.0$, given in Ref. [11]. The anomalous magnetic moment κ_{Λ^*} for the Λ^* amounts to 0.44 in the SU(3) quark model [11]. From the χ UM, it was also estimated to be $0.24 \sim 0.45$ [17]. Therefore, without loss of generality, we use $\kappa_{\Lambda^*} \approx 0.4$ for numerical calculations. The value of $g_{K^*N\Lambda^*}$ is chosen to be a free parameter, assuming that $|g_{K^*N\Lambda^*}| \leq g_{K\Lambda^*}$. The $g_{\gamma K K^*}$ can be computed from experiments and reads 0.388 GeV^{-1} for the neutral decay and 0.254 GeV^{-1} for the charged decay [14].

Having performed a straightforward calculation by using the effective Lagrangian given in Eq. (1), we obtain the invariant amplitudes for each diagram within the PS-coupling scheme as follows:

$$\begin{aligned} i\mathcal{M}_s &= -g_{K\Lambda^*}\bar{u}(p_2)\left[e_N\frac{\not{k}_1+\not{p}_1+M_N}{s-M_N^2}+\frac{e_Q\kappa_N(\not{p}_1+\not{k}_1+M_N)}{2M_N}\not{k}_1\right]\not{u}(p_1)\times F_{\gamma NN}F_{K\Lambda^*}, \\ i\mathcal{M}_u &= \frac{e_Q\kappa_{\Lambda^*}g_{K\Lambda^*}}{2M_{\Lambda^*}}\bar{u}(p_2)\not{k}_1\frac{(\not{p}_2-\not{k}_1+M_{\Lambda^*})}{u-M_{\Lambda^*}^2}u(p_1)\times F_{K\Lambda^*}F_{\gamma\Lambda^*\Lambda^*}, \\ i\mathcal{M}_t^K &= 2e_Kg_{K\Lambda^*}\bar{u}(p_2)\frac{(\not{k}_2\cdot\epsilon)}{t-m_K^2}u(p_1)\times F_{K\Lambda^*}F_{\gamma KK}, \\ i\mathcal{M}_t^{K^*} &= ig_{\gamma KK^*}g_{K^*N\Lambda^*}\bar{u}(p_2)\gamma_5\frac{\epsilon_{\mu\nu\sigma\rho}k_1^\mu\epsilon^\nu k_2^\sigma\gamma^\rho}{t-M_{K^*}^2}u(p_1)\times F_{K^*N\Lambda^*}F_{\gamma KK^*}, \end{aligned} \quad (2)$$

where the Mandelstam variables are $s = (k_1 + p_1)^2$, $u = (p_2 - k_1)^2$, and $t = (k_1 - k_2)^2$, while ϵ_μ the polarization vector for the incident photon. The form factors for the electromagnetic (EM) and hadronic vertices are given as:

$$F_{\gamma\Phi\Phi(BB)} = \frac{\Lambda_{\text{EM}}^2}{\Lambda_{\text{EM}}^2 + |\mathbf{k}_\gamma|^2}, \quad F_{\Phi BB} = \frac{\Lambda_h^2 - M_\Phi^2}{\Lambda_h^2 + |\mathbf{k}_\Phi|^2}, \quad (3)$$

where the subscripts Φ and B stand for the mesonic and baryonic particles involved, while M and \mathbf{k} are the on-shell mass and the three momentum for the relevant particles. The Λ_{EM} and Λ_h are the cutoff masses for the EM and hadronic form factors, respectively. In principle, the cutoff mass corresponds to the inverse size of a hadron approximately. In order to preserve the gauge invariance, since the u - and K^* -exchange channels are gauge-invariant by themselves, it is enough to take $F_{\gamma KK} = F_{\gamma NN}$, similar sizes being assumed for the proton ($\langle r^2 \rangle_p^{1/2} \approx 0.82 \text{ fm}$) and kaon ($\langle r^2 \rangle_{K^+}^{1/2} \approx 0.67 \text{ fm}$), approximately. Moreover, we also set $F_{K^*N\Lambda^*} = F_{K\Lambda^*}$ and $F_{\gamma K^*K} = F_{\gamma KK}$ for simplicity.

Assuming that the Λ^* can be regarded as a molecular-type $\bar{K}N$ bound state rather than a uds color-singlet state, one can infer that its size may be large in comparison to usual baryons such as the nucleon. In fact, we know from the phenomenological and chiral potential model calculations that the absolute value of the EM charge radius of Λ^* , $|\langle r^2 \rangle_{\Lambda^*}^{1/2}|$ was estimated as 1.36 fm [18] and 1.8 fm [19], respectively, and its value was estimated to be 1.48 fm [20] in the χ UM. These values are about two times larger than those of the typical baryons such as the proton $\sim 0.86 \text{ fm}$. Therefore, one may expect that the cutoff mass for the form factor for the $\gamma\Lambda^*\Lambda^*$ can be smaller than usual baryons, corresponding to its larger spatial size. Thus, we choose the cutoff mass for the EM form factor to be 650 MeV for the all vertices as done for the $\Lambda(1520)$ photoproduction [9], except for the $\gamma\Lambda^*\Lambda^*$ vertex in the u -channel, for which we employ $\Lambda_{\text{EM}} \approx 300 \text{ MeV}$, based on previous studies in various models. Although the cutoff mass for the hadronic form factors remain undetermined, we take it as the same as that for the EM ones for brevity, $\Lambda_h \approx 650 \text{ MeV}$. We note that choosing a different cutoff mass only for the $F_{\gamma\Lambda^*\Lambda^*}$ in the u -channel does not break the gauge invariance, since the u -channel amplitude is gauge-invariant by itself, as it contains only the magnetic coupling. All relevant parameters used in the present work are listed in Table I.

$g_{K\Lambda^*}$	$g_{K^*N\Lambda^*}$	κ_{Λ^*}	Λ_h	Λ_{EM}
3.18	$\pm 3.18, 0$	0.4	650 MeV	$650(300) \text{ MeV}$

TABLE I: Relevant coupling strengths and anomalous magnetic moment, and cutoff masses for the Λ^* photoproduction. The $\Lambda_{\text{EM}} = 300 \text{ MeV}$ is only for the electromagnetic form factor $F_{\gamma\Lambda^*\Lambda^*}$.

¹ Here we take the absolute value of the $g_{K\Lambda^*}$ computed in the χ UM, since it is a complex number in general at the pole.

III. NUMERICAL RESULTS

We now provide the numerical results of the total and differential cross sections, and the photon-beam asymmetry. First, we show those for the total cross section as a function of the photon energy E_γ in the left panel of Fig. 2. We consider three different values of the $g_{K^*N\Lambda^*}$ (0 and ± 3.18). The results indicate that the total cross section increases rapidly near the threshold, and then it starts to fall off slowly as the photon energy increases. We note that the s -channel contribution plays a main role in producing the present energy dependence, whereas other contributions start to be effective beyond about $E_\gamma = 1.7$ GeV. The K^* -exchange contribution interferes constructively (+3.18) and destructively (3.18) with other contributions, as depicted in Fig 2. The maximum value of the magnitude of the total cross section turns out to be $0.1 \lesssim \sigma_{\Lambda^*} \lesssim 0.2 \mu\text{b}$ near the threshold depending on the value of $g_{K^*N\Lambda^*}$. We note that, however, this tendency is rather different from that of the ground state $\Lambda(1116)$ photoproduction from the $\gamma p \rightarrow K^+ \Lambda(1116)$ reaction, in which the t -channel contribution is dominant to produce the appropriate energy dependence [7, 10]. In this sense, the t -channel dominance was argued that it also holds for the Λ^* photoproduction in Ref. [13] for instance. We note that, however, these different aspects are strongly dependent on the choice of the form factor schemes as will be discussed in Sec. IV.

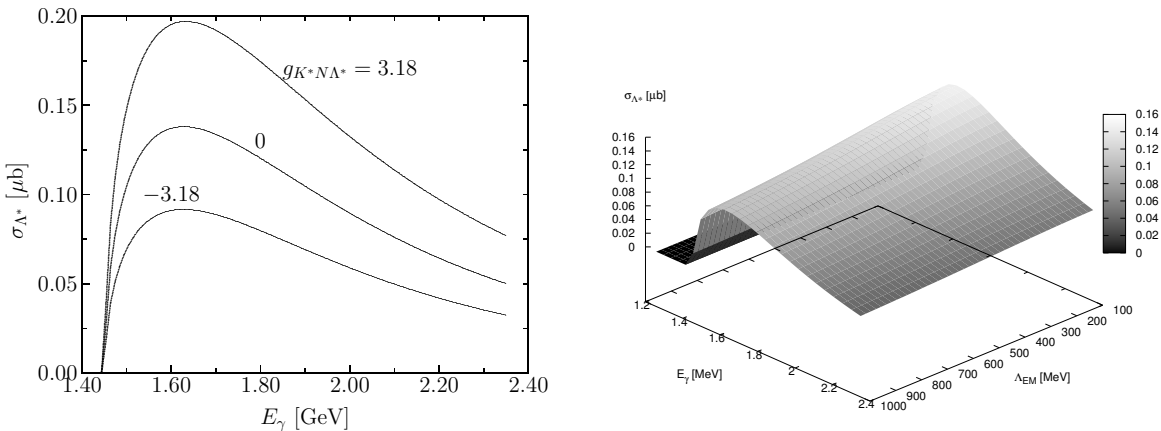


FIG. 2: In the left panel, the total cross section for the Λ^* photoproduction σ_{Λ^*} for the different coupling strengths of the $g_{K^*N\Lambda^*} \leq |g_{K^*N\Lambda^*}|$ are drawn as a function of the photon energy E_γ . Here, we use the $\Lambda_{\text{EM}} = 300$ MeV for the $F_{\gamma\Lambda^*\Lambda^*}$. In the right panel, the total cross section σ_{Λ^*} is represented as a function of both the cutoff mass Λ_{EM} for the $F_{\gamma\Lambda^*\Lambda^*}$ and the photon energy E_γ .

We are now in a position to discuss the size effect of the Λ^* . As mentioned in Sec. II, we examine this effect by introducing a phenomenological electromagnetic form factor $F_{\gamma\Lambda^*\Lambda^*}$, varying the cutoff mass Λ_{EM} that reflects the size of the hyperon. In the right panel of Fig. 2 we draw the total cross section for $g_{K^*N\Lambda^*} = 0$ as a function of the photon energy as well as of the cutoff mass Λ_{EM} for the $F_{\gamma\Lambda^*\Lambda^*}$. We observe that as the size of the Λ^* decreases (Λ_{EM} increases), the magnitude of the total cross section becomes larger around $E_\gamma \approx 1.6$ GeV due to the enhancement of the u -channel contribution. For instance, we can see from this figure that the maximum value of the total cross section is about $0.12 \mu\text{b}$ for the $\Lambda_{\text{EM}} = 650$ MeV, whereas about $0.13 \mu\text{b}$ for the $\Lambda_{\text{EM}} = 300$ MeV. Although we observe that the change in the total cross section depends on the size of the Λ^* , it is still small in comparison to theoretical ambiguities such as the $g_{K^*N\Lambda^*}$.

In a recent experiment for the $\gamma p \rightarrow K^+ \Lambda^*$ scattering process by the LEPS collaboration at SPring-8, it was shown that there is a large difference in the $\Lambda^*/\Sigma(1385)$ production ratio between the low ($1.5 \lesssim E_\gamma \lesssim 2.0$ GeV) and high energy ($2.0 \lesssim E_\gamma \lesssim 2.4$ GeV) regions [2]. This tendency may indicate that the energy dependence of the σ_{Λ^*} is qualitatively similar to our results as shown in the left panel of Fig. 2. Niyama et al. [2] also suggest that this interesting tendency may be caused by either the novel internal structure of the Λ^* or the different production mechanisms. From the present theoretical estimates, the s -channel dominance, being different from the usual t -channel one shown in the ground state $\Lambda(1116)$ photoproduction, must be responsible for this large difference in the ratio, whereas the size effect that encodes the novel internal structure of the Λ^* makes only small contribution.

In Fig. 3, we present the differential cross section as a function of $\cos \theta_{\text{cm}}$ in which the θ_{cm} denotes the angle between the incident photon and the outgoing kaon in the center of mass (cm) system. We also test the three different cases for the $g_{K^*N\Lambda^*} = 0$ (left), 3.18 (middle) and -3.18 (right), varying the photon energy E_γ from 1.45 GeV to 2.35 GeV. When the K^* -exchange contribution is excluded as shown in the left panel of the figure, the angular dependence shows the bump structure around $\cos \theta_{\text{cm}} \approx 0.75$, and it becomes noticeable as the photon energy increases. The main

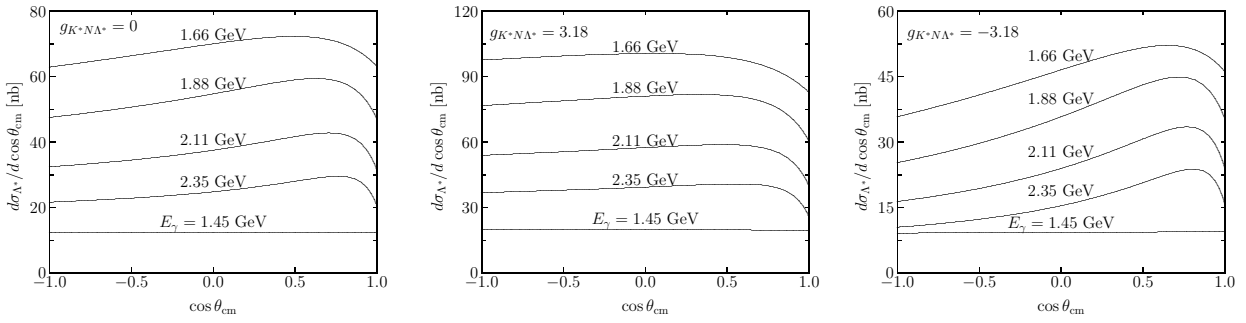


FIG. 3: Differential cross section $d\sigma_{\Lambda^*}/d \cos \theta_{\text{cm}}$ as a function of $\cos \theta_{\text{cm}}$. We also consider three different coupling strengths, $g_{K^*N\Lambda^*} = 0$ (left), 3.18 (middle) and -3.18 (right), varying the photon energy E_γ .

contributions to this bump are those of the s -channel and the t -channel, which enhance the differential cross section with the bump in the forward region. Note that the u -channel contribution turns out to be negligible.

For a finite $g_{K^*N\Lambda^*}$ as in the middle ($g_{K^*N\Lambda^*} = 3.18$) and right ($g_{K^*N\Lambda^*} = -3.18$) panels, the angular dependence of the differential cross section is changed obviously, since the K^* -exchange contributes mildly to the backward region. Due to the distinctive interference pattern between the K^* -exchange contribution and others, especially to the t -channel, the bump in the forward region gets diminished ($g_{K^*N\Lambda^*} = 3.18$) or enhanced ($g_{K^*N\Lambda^*} = -3.18$) in comparison to the case without the K^* -exchange. If we take a larger (smaller) value for the Λ_{EM} to test the size effect of the Λ^* , it turns out that only the magnitude of the curves become slightly smaller (larger), whereas the angular dependence remains almost the same, as expected from the results shown in the right panel of Fig. 2.

In Ref. [11], the differential cross section was computed for the $g_{K\Lambda} = 1.5$ and 3.0 with the nucleon-resonance contributions from $N^*(1650)$ and $N^*(1710)$. It showed a small forward-scattering enhancement, being similar to ours qualitatively, but the order of magnitude of the differential cross section in their work is about three or four times larger than ours when $g_{K\Lambda} = 3.0$. From the experimental data [2], the differential cross section was estimated to be about $0.4 \mu\text{b}$ for $1.5 \lesssim E_\gamma \lesssim 2.0 \text{ GeV}$ and $0.8 \lesssim \cos \theta_{\text{cm}} \lesssim 1.0$. This value is about four and two times larger than ours and that of Ref. [12], respectively, but very similar to that of Ref. [11], although all of them are in a similar order.

Now we define the photon-beam asymmetry, which is an important physical observable in the photoproduction, as follows:

$$\Sigma_{\Lambda^*} = \frac{d\sigma_{\Lambda^*\perp} - d\sigma_{\Lambda^*\parallel}}{d\sigma_{\Lambda^*\perp} + d\sigma_{\Lambda^*\parallel}}, \quad (4)$$

where the subscript \perp (\parallel) indicates that the incident photon is polarized transversely (longitudinally) to the reaction plane. We note that by definition the Σ_{Λ^*} becomes positive for the magnetic photon-hadron coupling contribution, whereas the negative for the electric one. We observe that the u -channel and K^* -exchange contributions give finite positive values for the Σ_{Λ^*} . On the contrary, it becomes -1 for the K -exchange, and negligible for the s -channel contribution.

In Fig. 4, we show the numerical results for the Σ_{Λ^*} as a function of $\cos \theta_{\text{cm}}$ varying the strength of the $g_{K^*N\Lambda^*} = 0, 3.18, -3.18$. We also alter the photon energy, $E_\gamma = 1.45 \text{ GeV} \sim 2.35 \text{ GeV}$. In Fig. 4, we observe that the Σ_{Λ^*}

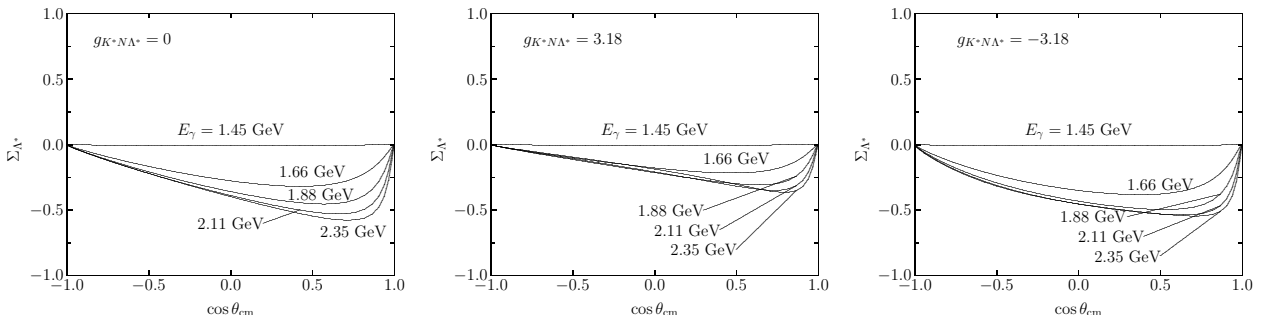


FIG. 4: Photon-beam asymmetry as a function of $\cos \theta_{\text{cm}}$. We also consider the three different coupling strengths, i.e. $g_{K^*N\Lambda^*} = 0$ (left), 3.18 (middle) and -3.18 (right) varying the photon energy E_γ .

becomes negative for all the cases due to the strong contribution of the electric coupling from the K -exchange. In the left panel of Fig. 4, we draw the results with $g_{K^*N\Lambda^*} = 0$. The Σ_{Λ^*} becomes tilted negatively in the forward region ($0.5 \lesssim \cos \theta_{cm}$) because of the destructive interference between the u -channel and K -exchange contributions. Even though we include the magnetic-coupling contributions such as the K^* -exchange, the qualitative shapes of the curves for the beam asymmetry remain almost unchanged as shown in the middle ($g_{K^*N\Lambda^*} = 3.18$) and right ($g_{K^*N\Lambda^*} = -3.18$) panels. It indicates that only small interferences with the K^* -exchange contribution appear. The photon-energy dependence of the Σ_{Λ^*} shows the mild enhancement of the bump around $0.5 \lesssim \cos \theta_{cm} \lesssim 1.0$, because of the u -channel contribution. We also verified that the size effect from the Λ^* is hard to be seen in the photon-beam asymmetry.

IV. DISCUSSIONS ON THEORETICAL AMBIGUITIES

In this Section, we want to discuss theoretical ambiguities, which may make significant effects on the present results given in Sec. III. We can consider the three theoretical ambiguities that are most critical in the present work:

- The coupling strengths of the $g_{K\Lambda\Lambda^*}$ and the $g_{K^*N\Lambda^*}$,
- The form factor scheme,
- The resonance contributions.

As explained in Sec. III, we have used the $g_{K\Lambda\Lambda^*} = 3.18$, which is derived by averaging the possible values of the $g_{K\Lambda\Lambda^*}$ computed from the χ UM with different regularization schemes, considering only the higher pole for the Λ^* which couples to the $\bar{K}N$ state strongly in comparison to the lower one. If we take the lower pole additionally, the coupling strength becomes smaller, $g_{K\Lambda\Lambda^*} = 2.6$. With this value, the maximum value of the total cross section gets lowered by about $30 \sim 40\%$. The phenomenological estimations [11], $g_{K\Lambda\Lambda^*} = 1.5 \sim 3.0$ can also give larger uncertainties but does not change the results much qualitatively, in particular, the energy dependence.

As for the $g_{K^*N\Lambda^*}$, the overall shapes of the total cross sections and the photon-beam asymmetry do not depend much on it within our present choice of the parameter range. On the contrary, the differential cross section (angular dependence) is affected by different values of the $g_{K^*N\Lambda^*}$ due to the complicated interference pattern between the K^* -exchange contribution and others. The other Λ hyperons being considered, the theoretical estimations of the ratio $|g_{K^*N\Lambda(1520)}/g_{K\Lambda\Lambda^*(1520)}|$ is very small ~ 0.1 [22]. On the other hand, the Nijmegen potential suggests $|g_{K^*N\Lambda(1116)}/g_{K\Lambda\Lambda^*(1116)}| \approx 5$ [23]. Thus, it is rather difficult to choose a reasonable value for $g_{K^*N\Lambda^*}$ from the phenomenological point of view. We also note that from the pure duality consideration as in Ref. [11], the K^* -exchange contribution can be ignored. If this is the case, we can assume that the $g_{K^*N\Lambda^*}$ is not large.

We can also choose the different schemes for the form factors as in Refs. [24–26]:

$$F(x) = \frac{\Lambda^4}{\Lambda^4 + (x - m_x^2)^2}, \quad (5)$$

where x and m_x stand for the Mandelstam variable and the intermediate hadron with the off-shell momentum squared $q^2 = x$, respectively. The Λ is the four-dimensional cutoff mass. The detailed explanation for its usage can be found in Refs. [10, 27]. This form factor preserves the Ward-Takahashi identity, and one of its typical features lies in the fact that it suppresses the s - and u -channel contributions, leading to the t -channel dominance, when it is applied to the spin-1/2 baryon photoproduction [10, 27]. In this case, the contributions from the s - and u -channels become small or negligible. Consequently, the angular dependence computed in this scheme usually shows a strong enhancement in the forward direction due to the t -channel. Especially, the t -channel contribution has been argued as the dominant one to reproduce the experimental data of the ground state $\Lambda(1116)$ photoproduction [7, 10, 28].

We draw the energy dependence in the left panel of Fig. 5 for the Λ^* photoproduction using the form factor given in Eq. (5) with the cutoff mass $\Lambda = 700$ MeV. As shown in Fig. 5, the total cross section increases slowly, starting from the threshold, and then becomes almost saturated in the vicinity of $E_\gamma \approx 2.2$ GeV. This tendency is very different from that shown in the left panel of Fig. 2 for which the form factors of Eq. (3) are used. We also have verified that the K^* -exchange brings out only a small deviation from the curve given in Fig. 5.

We now look carefully into these form factor schemes. In the right panel of Fig. 5 we depict the various form factors as a function of the photon energy which are applied to the invariant amplitudes in a gauge-invariant manner for the Λ^* photoproduction as follows:

$$\begin{aligned} i\mathcal{M}_{\text{total}}^{\text{Eq. (3)}} &= F_{\gamma BB(MM)} F_{MBB} [i(\mathcal{M}_s^E + \mathcal{M}_s^M) + i\mathcal{M}_t + i\mathcal{M}_u^M], \\ i\mathcal{M}_{\text{total}}^{\text{Eq. (5)}} &= [i(F_c \mathcal{M}_s^E + F_s \mathcal{M}_s^M) + iF_c \mathcal{M}_t + iF_u \mathcal{M}_u^M], \end{aligned} \quad (6)$$

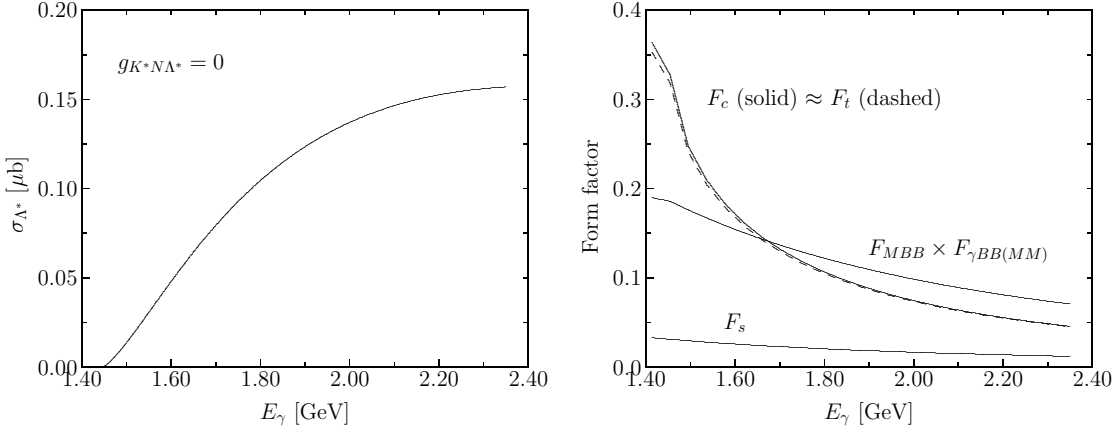


FIG. 5: In the left panel, we draw the total cross section as a function of the photon energy E_γ with the four dimensional gauge-invariant form factor given in Eq. (5). In the right panel, we depict the form factors given in Eqs. (3) and (5) as a function of the photon energy E_γ , respectively.

where we ignore the K^* -exchange contribution for simplicity. The \mathcal{M}_s^E means the electric part of the s -channel amplitude, whereas \mathcal{M}_s^M that of the magnetic one. Following Refs. [24–26], we can define the F_c as $F_s + F_t - F_s F_t$ so that it may satisfy the on-shell condition, $F(0) = 1$. From Fig. 5, we see that the F_c is almost the same as F_t , while the F_s is much smaller than them. The F_u is also negligible in comparison to the F_c . The $F_{\gamma BB(MM)} F_{MBB}$ lies between F_c and F_s . Hence, in the form factor scheme of Eq. (5), the differences between the channels become clear: The t -channel is effective much more than others. On the contrary, the form factor given in Eq. (3) suppresses all the channels simultaneously as the photon energy increases. Thus, the s -channel contribution can dominate the process near the threshold.

Finally, we may expect possible contributions from the nucleon, Δ and hyperon resonances, which have been excluded in the present work. For instance, Oh *et al.* [21] studied the $\Sigma(1385)$ photoproduction in a similar method to the present work, but with various resonance contributions, whose relevant coupling strengths to the $\Sigma(1385)$ were derived theoretically, the SU(3) relation being considered. From their analysis, it turned out that the resonance contribution plays an important role for the region from the threshold to $E_\gamma \approx 2$ GeV. If this is the case also for the Λ^* photoproduction, although they are different in the spin and parity, and information on the Λ^* related to the resonances is very poor in comparison to the $\Sigma(1385)$, the present results can be altered to a large extent.

V. SUMMARY AND CONCLUSION

In the present work, we have investigated the $\Lambda(1405, 1/2^-) \equiv \Lambda^*$ photoproduction, employing the effective Lagrangian approach in the Born approximation. We took into account the minimal contributions, the s - and u -channels, and the pseudoscalar K - and vector K^* -exchange contributions in the t -channel, without nucleon- and hyperon-resonance contributions such that the analysis of the $\Lambda(1405, 1/2^-)$ photoproduction mechanism can be easily achieved. All the necessary parameters were determined from the possible theoretical (the χ unitary model) and experimental (the $\Lambda(1520)$ photoproduction) results. The phenomenological electromagnetic and hadronic form factors were introduced with the gauge invariance preserved.

Assuming the molecular-type $\bar{K}N$ bound state for the Λ^* rather than the uds color-singlet one, we examined the size effect of the Λ^* by changing the cutoff mass for the electromagnetic form factor sitting on the $\gamma\Lambda^*\Lambda^*$ interacting vertex. Choosing this cutoff mass $\Lambda_{EM} \approx 300$ MeV, which may correspond to a larger spatial size of the Λ^* and is about a half of the other cutoff mass $\Lambda_h \approx 650$ MeV, we observed that, depending on the choice of the $K^*N\Lambda^*$ coupling strength, the total cross section turns out to be $0.1 \lesssim \sigma_{\Lambda^*} \lesssim 0.2 \mu b$ near the threshold and decreases slowly beyond $E_\gamma \approx 1.6$ GeV, showing the s -channel dominance. The angular dependence shows a mild enhancement in the forward direction due to the K -exchange in the t -channel. By the same reason, the photon-beam asymmetry resulted in the electric-coupling dominance (negative photon-beam asymmetry) for all angle regions.

Concerning the size effect of the Λ^* , had we considered its larger size, the bump at $E_\gamma \approx 1.6$ GeV shown in the total cross section would have increased slightly and smoothly, because of the enhancement of the u -channel contribution near the threshold. However, we note that the size effect is hard to be seen in all the physical observables computed in the present work. Consequently, we note that the enhancement of the total cross section near the threshold, as

reported by the LEPS experiment, can depend much on the different production mechanisms, as shown in Sec. III, not on the novel internal structure of the Λ^* .

Finally, we discussed the theoretical ambiguities which can make effects on the present results given in Sec. III. Among them, while the coupling strengths made little change the physical observables, it turned out that the form factor schemes are of great significance in the present results. The contributions from higher resonances may play also an important role in describing the mechanism of the Λ^* photoproduction. The corresponding works are under progress.

Acknowledgments

The authors would like to thank J. K. Ahn, T. Nakano, D. Jido, M. Niiyama, and H. Kohri for fruitful discussions. The work of H.C.K. is supported by Basic Science Research Program through the National Research Foundation of Korea (NRF) funded by the Ministry of Education, Science and Technology (grant number: 2009-0089525).

- [1] R. H. Dalitz, Eur. Phys. J. C **3** (1998) 676.
- [2] M. Niiyama *et al.*, Phys. Rev. C **78** (2008) 035202.
- [3] H. Fujimura [LEPS TPC Collaboration], AIP Conf. Proc. **915** (2007) 737 [Prog. Theor. Phys. Suppl. **168** (2007) 123].
- [4] M. Q. Tran *et al.* [SAPHIR Collaboration], Phys. Lett. B **445** (1998) 20.
- [5] D. P. Barber *et al.*, Z. Phys. C **7** (1980) 17.
- [6] S. Janssen, J. Ryckebusch, W. Van Nespen, D. Debruyne and T. Van Cauteren, Eur. Phys. J. A **11** (2001) 105.
- [7] S. Janssen, J. Ryckebusch, D. Debruyne and T. Van Cauteren, Phys. Rev. C **65** (2002) 015201.
- [8] L. Roca, E. Oset and H. Toki, arXiv:hep-ph/0411155.
- [9] S. i. Nam, A. Hosaka and H. -Ch. Kim, Phys. Rev. D **71** (2005) 114012.
- [10] S. Ozaki, H. Nagahiro and A. Hosaka, Phys. Lett. B **665** (2008) 178.
- [11] R. A. Williams, C. R. Ji and S. R. Cotanch, Phys. Rev. C **43** (1991) 452.
- [12] J. C. Nacher, E. Oset, H. Toki and A. Ramos, Phys. Lett. B **455** (1999) 55.
- [13] M. F. M. Lutz and M. Soyeur, Nucl. Phys. A **748** (2005) 499.
- [14] W. M. Yao *et al.* [Particle Data Group], J. Phys. G **33** (2006) 1.
- [15] S. i. Nam, H. -Ch. Kim, T. Hyodo, D. Jido and A. Hosaka, J. Korean Phys. Soc. **45** (2004) 1466.
- [16] D. Jido, E. Oset and A. Ramos, Phys. Rev. C **66** (2002) 055203.
- [17] D. Jido, A. Hosaka, J. C. Nacher, E. Oset and A. Ramos, Phys. Rev. C **66** (2002) 025203.
- [18] T. Yamazaki and Y. Akaishi, Phys. Rev. C **76** (2007) 045201.
- [19] T. Hyodo and W. Weise, Phys. Rev. C **77** (2008) 035204.
- [20] T. Sekihara, T. Hyodo and D. Jido, Phys. Lett. B **669** (2008) 133.
- [21] Y. Oh, C. M. Ko and K. Nakayama, Phys. Rev. C **77** (2008) 045204.
- [22] T. Hyodo, S. Sarkar, A. Hosaka and E. Oset, Phys. Rev. C **73** (2006) 035209 [Erratum-ibid. C **75** (2007) 029901].
- [23] V. G. J. Stoks and T. A. Rijken, Phys. Rev. C **59** (1999) 3009.
- [24] K. Ohta, Phys. Rev. C **40** (1989) 1335.
- [25] H. Haberzettl, C. Bennhold, T. Mart and T. Feuster, Phys. Rev. C **58** (1998) 40.
- [26] R. M. Davidson and R. Workman, Phys. Rev. C **63** (2001) 025210.
- [27] S. i. Nam, A. Hosaka and H. -Ch. Kim, J. Korean Phys. Soc. **49** (2006) 1928.
- [28] T. Hyodo, A. Hosaka, M. J. Vicente Vacas and E. Oset, Phys. Lett. B **593** (2004) 75.